Agricultural Water Management 109 (2012) 81–93

Contents lists available at SciVerse ScienceDirect

Agricultural Water Management

journal homepage: www.elsevier.com/locate/agwat

Evaluation of subsurface drip irrigation design and management parameters for alfalfa

Maziar M. Kandelous[a,*], Tamir Kamai[a], Jasper A. Vrugt[b], Jiří Šimůnek[c], Blaine Hanson[a], Jan W. Hopmans[a]

[a] Department of Land, Air and Water Resources, University of California, Davis, CA 95616, USA
[b] Department of Civil and Environmental Engineering, University of California, Irvine, CA 92697, USA
[c] Department of Environmental Science, University of California Riverside, CA 92521, USA

ARTICLE INFO

Article history:
Received 19 September 2011
Accepted 26 February 2012
Available online 17 March 2012

Keywords:
Alfalfa
Subsurface drip irrigation
Optimization
HYDRUS-2D
AMALGAM

ABSTRACT

Alfalfa is one of the most cultivated crops in the US, and is being used as livestock feed for the dairy, beef, and horse industries. About nine percent of that is grown in California, yet there is an increasing concern about the large amounts of irrigation water required to attain maximum yield. We introduce a conceptual framework to assist in the design and management of subsurface drip irrigation systems for alfalfa that maximize yield, while minimizing deep percolation water losses to groundwater. Our approach combines the strengths of numerical modeling using HYDRUS-2D with nonlinear optimization using AMALGAM and Pareto front analysis. The HYDRUS-2D model is used to simulate spatial and temporal distributions of soil moisture content, root water uptake, and deep drainage in response to drip-line installation depth and distance, emitter discharge, irrigation duration and frequency. This model is coupled with the AMALGAM optimization algorithm to explore tradeoffs between water application, irrigation system parameters, and crop transpiration (T_a), to evaluate best management practices for subsurface drip irrigation systems in alfalfa. Through analysis of various examples, we provide a framework that seeks optimal design and management practices for different root distribution and soil textures.

Published by Elsevier B.V.

1. Introduction

Alfalfa is one of the most widely cultivated crops in the world, and is used as livestock feed for the dairy, beef, and horse industries (Breazeale et al., 2000). The United States is the world's largest producer of alfalfa, with an annual value of about one billion dollars. About nine percent of all alfalfa produced in the United States is grown in California, with an average acreage of 360,000 ha (900,000 acres, Alfalfa's commodity fact sheet, 2011).

Because of California's semi-arid climate, irrigation is necessary to attain high yields. In California, about 1.2 billion m^3 of water is used to irrigate alfalfa each year, which is about 20% of California's developed water supply (Natural Resources Defense Council, 2001; Putnam et al., 2001). These large amounts of required irrigation water have encouraged the development and application of efficient irrigation systems. Hutmacher et al. (2001) reported a 20% increase in water use efficiency for alfalfa by using subsurface drip irrigation (SDI) rather than furrow irrigation. Another comparison between SDI and flood irrigation by Godoy et al. (2003) demonstrated that subsurface irrigation significantly improved the yield by about 25%, while using about 40% less water than flood irrigation. The study by Alam et al. (2002) showed that a well-designed SDI system can potentially decrease the volume of applied water by about 22%, while increasing the yield by 7%, compared to using a center pivot sprinkler system.

Alfalfa, a perennial crop, is harvested between 3 and 11 times throughout the year, depending on soil, irrigation practice, and climatic conditions. One of the biggest challenges in alfalfa production is the selection of irrigation design and management practices that maximize yield (and thus income), while simultaneously minimizing water losses. In addition, at harvesting times the soil surface should be sufficiently dry so that machinery can drive over the field without creating stressed root zone soil moisture conditions, allowing for quick re-growth of the cut alfalfa. In addition, the nonlinearity of soil–water–plant relationship makes it particularly difficult to find irrigation systems and strategies that maximize yield while simultaneously minimizing water losses. For all these reasons the optimal irrigation system and design practices are not immediately obvious for most climatic and soil conditions. A subsurface drip system, however, is ideally suited as it directly supplies water to the rooting zone at high frequency, allowing control of surface soil moisture required, for dry soil surface conditions prior

* Corresponding author.
E-mail address: mkandelous@ucdavis.edu (M.M. Kandelous).

0378-3774/$ – see front matter. Published by Elsevier B.V.
doi:10.1016/j.agwat.2012.02.009

Nomenclature

AW_{max}	maximum possible applied water [$L^3 L^{-2}$]
D	drip-line depth [L]
DP	deep percolation [$L^3 L^{-2}$]
DP_{max}	maximum possible deep percolation [$L^3 L^{-2}$]
ET_a	actual evapotranspiration [LT^{-1}]
ET_o	reference evapotranspiration [LT^{-1}]
ET_p	potential evapotranspiration [LT^{-1}]
f	irrigation frequency [T^{-1}]
FE	finite elements
h	soil water pressure head [L]
h_1, h_2, h_3, and h_4	parameters of Feddes uptake reduction function [L]
ID	irrigation duration [T]
$I1$	optimization scenario such that $\omega_D = \omega_L = \omega_{AW} = \omega_{DP} = 1$
$I2$	optimization scenario such that $\omega_D = 0$ and $\omega_L = \omega_{AW} = \omega_{DP} = 1$
$I3$	optimization scenario such that $\omega_D = \omega_{DP} = 0$ and $\omega_L = \omega_{AW} = 1$
ISA	irrigation scheduling Alfalfa model
$K(h)$	unsaturated hydraulic conductivity [LT^{-1}]
K_c	crop coefficient
K_s	saturated hydraulic conductivity [LT^{-1}]
L	drip-line distance [L]
l	shape parameter in the van Genuchten soil hydraulic functions
L_x	width of the soil surface associated with transpiration [L]
m	shape parameter in the van Genuchten soil hydraulic functions, $m = 1 - 1/n$
N	number of irrigation events
n	shape parameter in the van Genuchten soil hydraulic functions
OF_i	objective function (i)
Q	drip-line discharge [$L^3 L^{-1} T^{-1}$]
q	drip-line discharge [$L^3 L^{-2} T^{-1}$]
$R1$	optimization scenario using uniform root distribution
$R2$	optimization scenario using linear root distribution
$S(x,z)$	sink term [$L^3 L^{-3} T^{-1}$]
SDI	subsurface drip irrigation
S_e	effective saturation
S_p	potential root water uptake [$L^3 L^{-3} T^{-1}$]
t	time [T]
$T1$	optimization scenario using clay-loam soil
$T2$	optimization scenario using loam soil
$T3$	optimization scenario using sandy-loam soil
T_a	actual plant transpiration [LT^{-1}]
T_p	potential plant transpiration [LT^{-1}]
x	horizontal spatial coordinate [L]
z	vertical spatial coordinate [L]
$\alpha(h)$	Feddes' uptake reduction function
α_{VG}	shape parameter in the van Genuchten soil hydraulic functions
$\beta(x,z)$	normalized root density for any coordinate in the two-dimensional soil domain [L^2]
θ	volumetric water content [$L^3 L^{-3}$]
θ_r	residual water content [$L^3 L^{-3}$]
θ_s	saturated water content [$L^3 L^{-3}$]
Ω	root zone area [L^2]
ω_D, ω_L, ω_{AW}, ω_{DP}	weighting factors for D, L, AW, and DP in objective functions

to alfalfa cutting. We use detailed numerical soil water flow modeling with HYDRUS-2D (Šimůnek et al., 2008), combined with a multi-criteria optimization framework to determine optimal irrigation water management strategies for subsurface drip irrigation of alfalfa.

Past sensitivity analysis (Gärdenäs et al., 2005) has shown that the root distribution exerts strong influence on subsurface drip irrigation design and management practices, as water uptake by plant roots determines spatial and temporal patterns in soil water availability. Whereas various past studies investigated root distributions of alfalfa (Abdul-Jabbar et al., 1982; Meinzer, 1927), we know of no studies that evaluate the effects of SDI on alfalfa root distribution.

The ever increasing pace of computational power along with significant advances in numerical modeling of soil–plant–water relationships enables the application of numerical vadose zone simulation models for analyses of micro-irrigation systems involving a wide range of crops. The HYDRUS-2D (Šimůnek et al., 2006, 2008) model has been widely used for this purpose, including for SDI (Gärdenäs et al., 2005; Hanson et al., 2006; Skaggs et al., 2006; Hanson et al., 2008). The effect of different irrigation design variables such as drip-line distance and drip-line installation depth can be readily simulated by such a modeling system for a range of soil types. Whereas these design parameters are relevant to water availability for crops and soil types, drip-line depth and distance also have economic consequences as they essentially determine irrigation system costs. Other factors to consider are leaching losses, rodent damage, and requirement of soil dryness before harvesting.

In this study, we present a general purpose multi-criteria optimization framework to help in the design of optimal subsurface drip irrigation systems for alfalfa. Instead of providing specific irrigation system and water application recommendations, we present a flexible optimization tool that allows definition of a range of objective functions to be minimized, using multiple criteria and weights. Our approach combines the strengths of numerical vadose zone modeling using HYDRUS-2D with the AMALGAM evolutionary search (Vrugt and Robinson, 2007) and Pareto front (Wöhling et al., 2008) algorithms, to provide water application strategies that maximize yield and minimize water loss for a range of irrigation system designs. In particular, we seek to optimize drip-line installation depth and distance, irrigation duration, and irrigation frequency, while maximizing root water uptake and minimizing irrigation water losses by leaching. In addition, our analysis is especially designed to ensure sufficiently dry soil surfaces at harvesting times. These optimal parameters are determined for different root distribution (uniform and linear), and soil types (sandy loam, loam, and clay loam). We realize that economics of irrigation system and water costs should also be considered, however, we do not consider these factors in the present analysis, as dollar values can be easily included in the formulation of the objective functions when available.

2. Materials and methods

A schematic of the followed computational procedures to arrive at the final set of optimal design and decision parameters is shown in the flow chart of Fig. 1. The main computational loop is defined by the AMALGAM evolutionary search algorithm (Vrugt and Robinson, 2007), selecting specific values of drip-line installation depth (D) and distance (L), irrigation duration (ID) and frequency (f) from

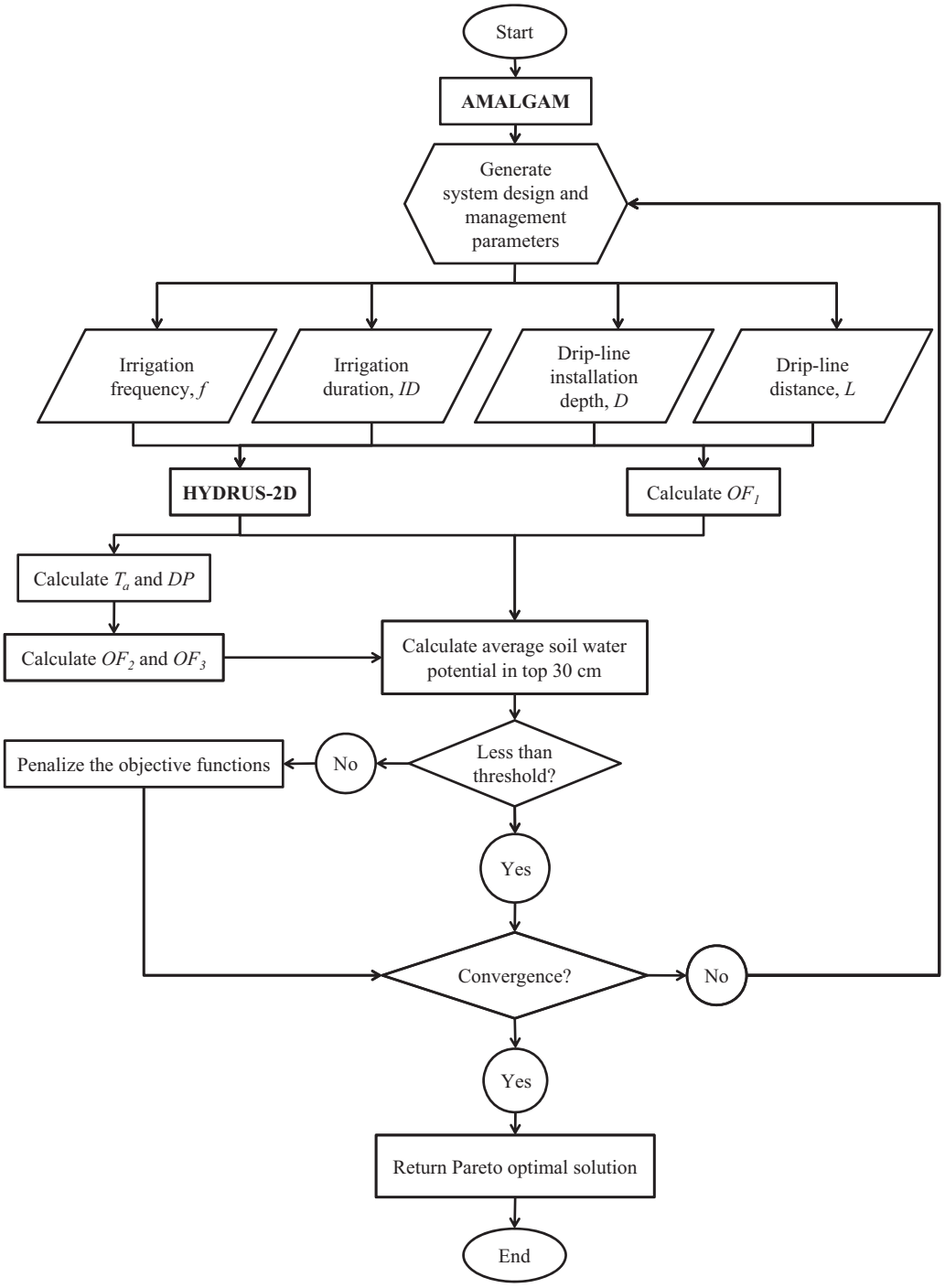

Fig. 1. Flow diagram of the presented multi-objective optimization approach. In this diagram, T_a denotes actual transpiration, *DP* is deep percolation, and OF_i represents the objective function *i*.

the prior allowed ranges (Table 1). For each of the selected combinations, the HYDRUS-2D unsaturated water flow model (Šimůnek et al., 2008) simulates soil water flow for the specific irrigation system selected and computes the spatial and temporal distributions of soil water potential and water content, with corresponding root water uptake, and drainage and actual transpiration rates for the growing season. In addition, cumulative values of actual transpiration (T_a), deep percolation losses (*DP*), and average soil water pressure head values for the top 30-cm at predefined harvesting times are computed for each growing season simulation. Upon completion of each HYDRUS simulation, AMALGAM evaluates the three objective functions (*OF*'s) of Eqs. (8) or (9) with

Table 1
Ranges of system design and water application parameters for HYDRUS model simulations, as defined for AMALGAM search algorithm.

	Lower value	Upper value	Interval
Drip-line depth (cm), *D*	20	70	5
Drip-line distance (cm), *L*	40	300	10
Duration of irrigation (h), ID	8	24	1
Irrigation frequency (days^{-1}), *f*	1/7	1	1/7

corresponding weighting factors (Eq. (8) only), and uses the *OF*-values to seek new system design parameters from the prior allowed ranges for a next iteration with HYDRUS-2D calculations. It is here where the AMALGAM search algorithm is novel and efficient, in seeking all possible optimal solutions with a minimum number of HYDRUS-2D simulation iterations required. Upon completion of the optimization, as determined by various pre-defined convergence criteria, AMALGAM derives the Pareto solution set that consists of a sample of optimal solutions representing different tradeoffs to the multi-criteria optimization problem. For this study of alfalfa subsurface drip irrigation, the main tradeoffs are between water application and transpiration. As an example of these complex trade-offs, for large distance between drip-lines more water must be applied in order to wet the root zone and satisfy non-stress conditions for high transpiration. However, adding more water to the root zone also increases deep percolation, whereas other parameters such as drip-line installation depth also influence transpiration and deep percolation. Thus, we seek a balance between the different processes and parameters. This trade-off balance is achieved by the Pareto front analysis, and provides for development of optimal subsurface drip irrigation system parameters for a range of soil types (Table 2) and typical root distributions. In the following we provide a detailed description of the various elements of our optimization framework. Although we limit our attention to alfalfa, the methodology presented herein can readily be applied to develop efficient drip irrigation designs for a wide range of crops.

2.1. Numerical HYDRUS simulations

The two-dimensional module of the HYDRUS-2D/3D package (Šimůnek et al., 2008) was used to simulate soil water movement and plant root water uptake for the specific irrigation system design and water application parameters defined in Table 1.

2.1.1. Soil water movement

The HYDRUS-2D model uses the two-dimensional form of Richards' equation to describe transient water flow in isotropic unsaturated soils:

$$\frac{\partial\theta}{\partial t} = \frac{\partial}{\partial x}\left[K(h)\frac{\partial h}{\partial x}\right] + \frac{\partial}{\partial z}\left[K(h)\frac{\partial h}{\partial z} + K(h)\right] - S(h) \quad (1)$$

where θ is the soil's volumetric water content [$L^3\,L^{-3}$], h denotes the soil water pressure head [L], $S(h)$ is a sink term [$L^3\,L^{-3}\,T^{-1}$] representing plant root water uptake, t signifies time [T], $K(h)$ is the unsaturated hydraulic conductivity function [LT^{-1}], and x and z are the horizontal and vertical spatial coordinates [L], respectively, of the simulated soil domain. Solution of Eq. (1) requires characterization of the soil hydraulic properties, as defined by the soil water retention, $\theta(h)$, and unsaturated hydraulic conductivity function, $K(h)$. We used the constitutive relationships of van Genuchten-Mualem (van Genuchten, 1980) and represent the effective saturation, S_e by:

$$S_e = \frac{\theta - \theta_r}{\theta_s - \theta_r} = \frac{1}{(1 + |\alpha_{VG}h|^n)^m} \quad (2)$$

and

$$K(h) = K_s S_e^l \left[1 - (1 - S_e^{1/m})^m\right]^2, \quad (3)$$

where θ_s and θ_r represent the saturated and residual water content [$L^3\,L^{-3}$], respectively, K_s is the saturated hydraulic conductivity [LT^{-1}], α_{VG} [L^{-1}], n, and l are shape parameters, and $m = 1 - 1/n$. Though these four parameters are directly related to pore size distribution, pore connectivity and tortuosity, they are generally obtained from fitting of $\theta(h)$ and $K(h)$ data to functions (2) and (3), respectively. Eq. (1) is solved using a Galerkin type linear finite element method applied to a network of triangular elements. Time integration is achieved using an implicit (backwards) finite difference scheme, with the approximate equations solved iteratively and time steps adjusted depending on convergence rates.

2.1.2. Root distribution and crop water uptake

The spatial distribution of the plant roots of alfalfa exerts a strong influence on soil water flow, root water uptake, and deep drainage, and therefore essentially determines *DP* and T_a for a given irrigation strategy. In the absence of detailed information about the spatial distribution of alfalfa roots in the literature, we assumed two different root distributions (linear and uniform), and conducted simulations for each of these two cases. Specifically, we used the sink term, $S(h)$, in Eq. (1) to quantify root water uptake, using the commonly used approach of Feddes et al. (1976):

$$S(h) = \alpha(h) \times S_p, \quad (4)$$

where $\alpha(h)$ is a dimensionless root water uptake reduction function with values between zero and one, to account for soil water stress. If the soil maintains favorable conditions for root water uptake, $S(h)$ is equal to the potential root water uptake rate, S_p [$L^3\,L^{-3}\,T^{-1}$]. However, if the soil is too dry or too wet at any given location (x,z), then $\alpha < 1$, and the uptake at position (x,z) is linearly reduced with the magnitude determined by the reduction function parameters for alfalfa as selected from a data-base (Taylor and Ashcroft, 1972). The potential root water uptake rate, S_p, is calculated from (Šimůnek and Hopmans, 2009):

$$S_p(x, z) = \beta(x, z)L_x T_p, \quad (5)$$

where $\beta(x,z)$ [L^{-2}] represents the normalized root density for any coordinate in the two-dimensional soil domain, L_x [L] denotes the width of the soil surface associated with the potential plant transpiration, T_p [LT^{-1}]. We note that the actual plant transpiration, T_a [LT^{-1}], is computed in HYDRUS-2D by numerical integration of Eq. (4) across the entire root zone, Ω [L^2], or:

$$T_a = \frac{1}{L_x}\int_\Omega S(h, x, z)d\Omega = \frac{1}{L_x}\int_\Omega \alpha(h)S_p(x, z)d\Omega, \quad (6a)$$

Substituting Eq. (5) into (6a), yields:

$$T_a = T_p \int_\Omega \beta'(h, x, z)d\Omega, \quad (6b)$$

where $\beta'(h, x, z) = \alpha(h) \times \beta(x, z)$.

Potential evapotranspiration of alfalfa was calculated using the irrigation scheduling alfalfa (ISA) model. This management model was especially developed to help determine a suitable irrigation strategy for alfalfa and to predict the effect of water stress on yield (Snyder and Bali, 2008). This model implements a standardized method for estimating reference evapotranspiration, ET_o (Allen et al., 1998, ASCE, 2005) and uses the crop coefficient, K_c, to compute potential daily evapotranspiration, ET_p, (Doorenbos and Pruitt, 1977), or

$$ET_p = ET_o \times K_c. \quad (7)$$

The K_c value varies during the growing season and depends on the length of initial, rapid, midseason and late growth stages. To illustrate this approach, we consider Fig. 2, presenting daily ET_p as calculated by the ISA model for a typical growing season of alfalfa, from March 1 (day 0 in Fig. 2) to October 26 (day 240 in Fig. 2) in the Sacramento Valley, USA (B.R. Hanson, unpublished data). As illustrated in Fig. 2, ET_p varies widely during the growing season, with K_c values ranging between near zero (after each cutting) and maximum values near 1.0 in the mid season. Because of full soil

Table 2
Soil hydraulic function parameters for soils of scenarios *T*1 (clay loam), *T*2, (loam) and *T*3 (sandy loam), as taken from Carsel and Parrish (1988).

	θ_r (cm^3 cm^{-3})	θ_s (cm^3 cm^{-3})	α_{VG} (cm^{-1})	n	K_s (cm day^{-1})	l
Clay loam	0.095	0.41	0.019	1.31	6.24	0.5
Loam	0.078	0.43	0.036	1.56	24.96	0.5
Sandy loam	0.065	0.41	0.075	1.89	106.1	0.5

coverage by the alfalfa, soil evaporation can be considered negligible throughout the simulated growing season, so that T_p in Eqs. (5) and (6) is equal to ET_p. Typically, the alfalfa is cut about once a month, starting in late April, through late October, for a total of 6 cuttings. In HYDRUS-2D, this time series of ET_p defines the potential root water uptake rate, S_p. We assumed a growing season with a total of six growing cycles, corresponding with the six cuttings. Despite the expected variations in alfalfa yield for the wide range of irrigation system parameters analyzed, the alfalfa cutting dates were held fixed to these same dates (Fig. 2) for all simulations.

2.1.3. Domain properties and boundary conditions

In all HYDRUS-2D simulations we assumed that the soil is homogeneous and that a drip-line behaves as an infinite line source with a constant water discharge rate along the drip line. Water flow in a homogenous soil is symmetrical in the horizontal direction between drip lines, so that only one-half of the domain space between drip-lines needs to be simulated. Therefore, the two-dimensional transport domain (Fig. 3) is rectangular, and $L/2$ cm wide (a half-length between drip-lines). We simulated a soil domain with a depth of 200 cm, and placed the subsurface drip line at depth D (right side of the domain). In each numerical simulation we assumed that the maximum rooting depth of alfalfa was similar to 200 cm, the bottom boundary of our hypothetical soils (Table 2). The spatial domain was discretized using triangular finite elements (FE). Depending on drip-line distance, L, the number of elements varied between 1954 and 4897, with element size gradually increasing with distance from the drip-line. The smallest FE size of 0.1 cm was selected around the drip-line, whereas the large FE's were about 5 cm, furthest away from the drip line. A high nodal density is required in the immediate vicinity of the drip-lines to be able to accurately model the large spatial gradients in soil water pressure head caused by the infiltrating water.

A time-variable flux boundary condition was used along the boundary elements representing the emitter, so that the total drip emitter discharge when integrated around the emitter was equal to the defined emitter discharge, q (volume per unit emitter area and time) (Gärdenäs et al., 2005). A free drainage (unit gradient) boundary condition was applied along the bottom boundary, allowing for downward drainage and leaching. All other remaining boundaries were assigned a zero water flux condition. Irrigation system design parameters were optimized using HYDRUS-2D simulations for a sandy loam, loam and clay loam soil type, with van Genuchten–Mualem soil hydraulic parameters of Eqs. (2) and (3) listed in Table 2.

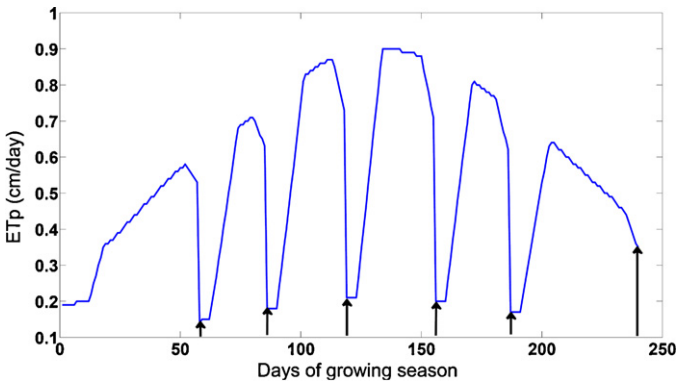

Fig. 2. Assumed alfalfa *ETp* using ISA model during simulated growing season. The arrows indicate the different cutting times.

2.2. Parameter optimization

Optimal irrigation system design and water application must maximize root water uptake and T_a, while minimizing total irrigation system installation costs, applied irrigation water and drainage water losses. For that purpose we optimized drip line depth (D) and distance (L), irrigation frequency (f), and irrigation duration (ID), with the latter two parameters enabling minimization of applied irrigation water (AW) using a fixed emitter discharge rate. The HYDRUS-2D model computes T_a, DP losses, and the near surface soil water content at the alfalfa cutting times for each of the selected parameter sets for each of the AMALGAM iterations, until it converges. In the final step, the search algorithm derives the Pareto solution set, consisting of a number of optimal solutions that each represents a different trade-off between various optimal irrigation system design parameters. The trade-offs are the result of minimizing three objective functions in Eqs. (8) or (9), and allows for selecting the optimal combination of parameters depending on relevance or cost differences between them. Hence, there is no single optimum parameter set, but the Pareto analysis provides for many combinations of parameter values that in combination result in similar residual values for the three combined objective functions.

Typically, parameter optimization methods such as AMALGAM are used to determine optimal parameter values by minimizing residuals between measured and model-simulated variables. However, in the present study, the objective functions are defined by minimizing residuals consisting of differences between optimum and model parameter/variable values, as defined in Eqs. (8) and (9). In some way, one can view our study as a sensitivity analysis, evaluating the impact of variable irrigation system design and

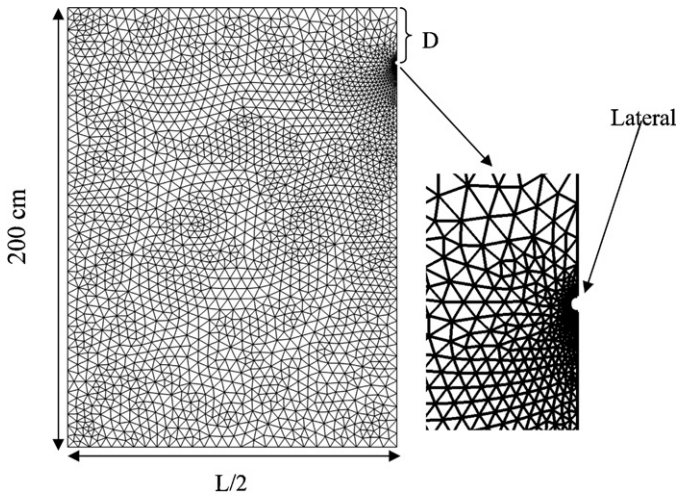

Fig. 3. Schematic overview of the two-dimensional numerical grid used by HYDRUS-2D for the presented simulations.

water application parameters on water use efficiency, defined by the ratio of AW to T_a.

2.2.1. Irrigation system parameters

The optimized irrigation system design and water application parameters with their upper and lower bound values are listed in Table 1. These parameters define the width of the prior uniform distribution functions from which selected parameter values are taken in the AMALGAM optimization procedure. They include the drip-line installation depth, D (L), drip-line distance, L (L), irrigation duration, ID (T), and irrigation frequency, f (T^{-1}). As each of these four parameters are expected to largely affect soil water flow, root water uptake, and drainage, we assumed physically realistic ranges, and used AMALGAM to find Pareto optimal solutions that simultaneously minimize the three different objectives considered in Section 2.2.2. In essence, we seek optimum combinations of D, L, ID and f, that maximize irrigation efficiency (as defined by minimizing applied water (AW) and deep percolation (DP) losses) and T_a. Without a preference to any of the individual objective functions (OF's) in the applied multi-criteria optimization analysis, the minimum uncertainty that can be achieved for the optimized parameters is essentially determined by the trade-off in minimizing the three different objectives. Specifically, if two objectives are conflicting, it is not possible to find a single combination of parameter values that optimizes both of these two objectives simultaneously. Instead, a trade-off will be determined in the fitting of both multiple objectives, resulting in parameter variations. The Pareto solution set defines the trade-offs with minimum OF values.

With regard to finding the optimum drip line depth (D), the near-surface soil must become sufficiently dry for each cutting operation, without reducing crop yield. On the other hand, a too large installation depth may cause deep percolation losses and increase installation costs. Whereas increasing drip-line distance is cost-effective, a too large spacing may require higher irrigation frequency to maintain optimum root zone soil moisture conditions between the drip lines, and increase drainage losses by deep percolation as a result. Similarly, large irrigation duration values will affect deep drainage and may cause plant water stress by introducing anaerobic soil conditions, thereby reducing T_a and yield. On the other hand, applying irrigation water at values less than T_p may reduce plant transpiration and yield even more. Therefore, irrigation frequency and/or water application duration must be higher in summer months compared to the early and late growing season. However, rather by varying irrigation frequency during the growing season, we chose to vary irrigation water application time, using average T_p rates for each of the six cutting cycles. In all our calculations reported herein, we assume a constant drip-line discharge per unit length, $Q = 2.3 \times 10^{-3}\ m^3\ m^{-1}\ h^{-1}$ (Alam et al., 2002).

Initial AMALGAM optimizations demonstrated the need for the finite element (FE) size of HYDRUS-2D domain to be flexible, to accommodate different irrigation designs and to minimize numerical model errors. For example, each combination of drip-line distance (L) and drip-line installation depth (D) required a different two-dimensional nodal discretization in HYDRUS-2D. For that purpose, we defined discrete drip installation depth (D) and drip line distance (L) increments of 5 and 10 cm, respectively (Table 1). We followed a similar approach for irrigation duration (ID) and frequency (f) parameters, and used 1-hour and 1-day time increments interval, respectively. While this approach significantly increased the efficiency of the multi-criteria analysis, it did not affect the final outcome.

2.2.2. Objective functions

For general application, we define the following three objective functions to be minimized, OF_i ($i = 1, 2, 3$), which in combination optimize irrigation system cost and benefit by minimizing drip-line depth (D), applied irrigation water (AW), and deep percolation (DP), while maximizing root water uptake and crop transpiration (T_a) and distance between irrigation drip-lines (L):

$$\begin{aligned} OF_1 &= \frac{1}{\omega_L + \omega_D} \times \left[\omega_D \frac{(D - D_{\min})}{(D_{\max} - D_{\min})} + \omega_L \left(1 - \frac{(L - L_{\min})}{(L_{\max} - L_{\min})} \right) \right] \\ OF_2 &= \frac{1}{\omega_{AW} + \omega_{DP}} \times \left[\omega_{AW} \frac{AW - AW_{\min}}{AW_{\max} - AW_{\min}} + \omega_{DP} \frac{DP - DP_{\min}}{DP_{\max} - DP_{\min}} \right], \\ OF_3 &= 1 - \frac{T_a}{T_p} \end{aligned} \tag{8}$$

The weighting factors ω_D, ω_L, ω_{AW}, and ω_{DP} allow to differentiate between cost of the decision variables within each objective function. In particular, ω_D denotes the cost of installation per unit depth, ω_L signifies the cost of unit length of drip-line, ω_{AW} is the cost of unit volume of water, and ω_{DP} represents either the cost of unit volume of water or the cost needed for disposing the unit volume of drained water. Realizing that minimum values of both DP and AW are zero and that $DP_{max} = AW_{max}$, each of the three objective functions are scaled functions with values ranging between zero and one.

The first objective function to be minimized, OF_1, minimizes the installation cost and equipment (i.e., drip-line) expense by minimizing the drip-line depth (D), while simultaneously maximizing the distance between drip-lines (L). This performance measure is solely dependent on the actual values of L and D and does not require a HYDRUS-2D run to calculate soil moisture dynamics. The second objective function, OF_2, minimizes the cost of water by minimizing the applied irrigation water (AW) and drainage water losses by deep percolation (DP). The third objective function, OF_3, maximizes the yield profit by minimizing soil water stress to maximize plant transpiration. These latter two criteria can be computed only using HYDRUS-2D. Differential weighting allows flexibility in applying the objective functions to different costing scenarios, if applicable. For example, in OF_1 one can assign the cost of installation and equipment for the known specified region or even select either D or L as the main decision parameter by assigning a zero weight to the specific parameter, if appropriate. We note that assigning a zero weight to a parameter excludes it as an objective function parameter, however, it will remain a variable parameter with an identified range (Table 1), thereby contributing to the Pareto distribution of optimized parameters.

For most of the analysis in this study, we simplified the three objective functions of Eq. (8) by eliminating the cost factor, and instead defined the combined objectives such as to optimize irrigation system parameters by minimizing applied irrigation water (AW), while maximizing root water uptake and crop transpiration (T_a) and distance between irrigation drip-lines (L):

$$\begin{aligned} OF_1 &= 1 - \frac{(L - L_{\min})}{(L_{\max} - L_{\min})} \\ OF_2 &= \frac{AW - AW_{\min}}{AW_{\max} - AW_{\min}}, \\ OF_3 &= 1 - \frac{T_a}{T_p} \end{aligned} \tag{9}$$

where $AW = q \times ID \times N$ with N representing the number of irrigations of duration ID and drip-line discharge q (LT^{-1}). Conveniently, each of the three objective functions are scaled functions with values ranging between zero and one. The first objective function to be minimized, OF_1, now maximizes the distance between drip-lines (L). The second objective function, OF_2, minimizes applied irrigation water (AW) and the third objective function, OF_3, seeks to maximize plant transpiration by minimizing soil water stress. The first two performance measures can be calculated directly from the parameters considered herein and hence do not require HYDRUS-2D simulations. Only for the third criteria, simulated soil moisture dynamics are required.

Minimization of objective functions in (Eq. (9)) might lead to physically unrealistic results. We therefore introduce two main constraints. First, only those solutions were accepted for which T_a was equal or higher than 85% of T_p. Available data indicated that alfalfa yields were only slightly affected for such a reduction, but that significant yield losses may occur for lower T_a values. Because of uncertainties in crop water production function (Grismer, 2001), which is depended on irrigation management and climatic region, we set the minimum acceptable value for T_a at 85% of T_p. Second, cutting of the alfalfa crop requires that the average soil water pressure potential in the top 30 cm is lower (more negative) than the prescribed threshold value of −500 cm, (B.R. Hanson, unpublished data) to allow cutting and baling machinery to drive on the field without destroying soil structure and crop. If one of the constraints was violated we penalized the corresponding objective functions so that these solutions were not further considered during the Pareto search. In general, values for both constraints can be changed for specific crops and irrigation water management applications.

2.2.3. AMALGAM method

In the presence of multiple conflicting objectives, it is highly unlikely that a single optimal parameter combination exists that satisfies all objectives. Instead, it is expected that a multi-criteria optimization will result in considerable trade-offs, as with multiple optimal parameter combinations, as defined by Pareto fronts (in case of two objectives) or Pareto surfaces (three or more objectives). The AMALGAM evolutionary search method of Vrugt and Robinson (2007) was used to explore the multiple parameter space and to provide the Pareto solutions using a very computational-efficient algorithm. A detailed explanation of this approach can be found in Vrugt and Robinson (2007) and Vrugt et al. (2009), and is beyond the scope of the current work. In brief, AMALGAM runs multiple different optimization methods simultaneously that each learns from each other using a common population of parameter values. The combination of optimization methods included in AMALGAM are Genetic Algorithm, Particle Swarm Optimizer, Differential Evolution, and Random Walk Metropolis with adaptive updating of the parameter covariance matrix. Improved parameter sets are generated in an iterative way, with each algorithm contributing in proportion to its convergence rate towards a final optimal parameter set. This approach has proven to be a credible and computationally efficient optimization model, especially if many parameters are optimized simultaneously. It has shown to significantly improve the efficiency of Pareto optimization, and is finding increasing use in many different study fields (e.g., Huisman et al., 2010).

2.3. Example scenarios

To illustrate the generality of the irrigation design approach, we present three different sensitivity analyses with identical climatic conditions and design constraints (Section 2.2.2.) to evaluate the effect of (1) selected irrigation parameters (*I*1, *I*2, and *I*3), (2) root distribution (*R*1 and *R*2), and (3) soil texture (*T*1, *T*2, and *T*3) on system design and management (Table 3).

The effect of irrigation system parameter type on the optimization results was investigated using three different scenarios considering simulations for the loam soil with uniform root distribution. For scenario *I*1, we evaluated the optimization results for the case that minimizes drip-line depth (*D*), *AW* and *DP*, while maximizing drip-line distance (*L*) and plant transpiration (T_a). In other words, scenario *I*1 minimizes the cost of installation, equipment, and water, while maximizing profit. We note that the main objective functions used in this study are those presented in Eq. (8), but here we show the generality of the presented method by assigning the arbitrary cost of unity for all decision parameters. Scenario *I*2 is the same as *I*1, except that we excluded the parameter *D* from the analysis ($\omega_D = 0$), as drip installation costs for the founded range in this study are almost independent of installation depth (Toro, Inc., personal communication). Scenario *I*3 is the same as *I*2, except we excluded *DP* as an optimization parameter ($\omega_{DP} = 0$), in addition, thus optimizing solely on maximum drip-line distance, *L* (OF_1) (minimizing installation costs), and minimizing plant water stress (OF_3) (maximizing plant transpiration, T_a, and crop yield), while applying a minimum amount of applied irrigation water, *AW* (OF_2).

It has been shown before that depth distribution of roots and associated root water uptake has a major influence of the soil water regime in micro irrigation (Gärdenäs et al., 2005; Hanson et al., 2008). However, since information on alfalfa root distribution in subsurface drip irrigation is absent, for the purpose of this optimization study we assumed two likely distribution functions that describe a (1) uniform and constant root distribution across the root zone (*R*1), and (2) linear decreasing rooting pattern with soil depth (*R*2). For the linear model, the maximum root density is at the soil surface and decreases linearly to a zero value at the bottom of the root zone. To minimize the number of optimizations for the root distribution analysis, we limited the optimizations to those for a loam soil only, setting ω_D in Eq. (8) equal to zero. Moreover, we set ω_{DP} in Eq. (8) to zero, to focus the analysis on minimizing applied water (*AW*) and maximizing drip-line separation distance (*L*) and plant transpiration (T_a).

The soil textural and hydraulic properties affect irrigation design and management due to their effect on horizontal, downward and upward vertical water movement. Therefore, three soil textures—clay loam (*T*1), loam (*T*2), and sandy loam (*T*3)–were considered in this study, evaluating the effect of soil hydraulic properties (Table 2) on irrigation design and management, for soil domains with a uniform root distribution only.

3. Results and discussion

To better understand the results of a multi-criteria parameter optimization with AMALGAM, we present the Pareto contour plot of Eq. (9) for a loam soil and uniform root distribution in Fig. 4a, with corresponding two-dimensional bi-criterion plots for the three-objective optimization in Figs. 4b–d. As described in Section 2.2.2, the multi-objective optimization approach used herein maximizes drip-line distance (*L*, OF_1) and crop transpiration (T_a, OF_3), minimizing applied irrigation water (*AW*, OF_2). In this specific application, the drip line installation depth, *D*, was excluded from OF_1, but their values are represented among the Pareto data points. Both the contour plot and 2-dimensional Pareto graphs present values for optimum parameters, with both *AW* and T_a normalized with respect to T_p. This final optimum parameter space is relatively small, because only limited water stress is allowed ($T_a/T_p > 0.85$), while simultaneously requiring dry soil conditions at all six cutting times, as achieved by penalizing the objective functions if either constraint is not satisfied.

We clarify that all data points of Fig. 4b–d combined, makeup the Pareto contour plot of Fig. 4a, with each data point representing a different Pareto optimal solution for any of the four design parameters combinations used in HYDRUS for which the two design constraints were satisfied. Specifically, the contour plot of Fig. 4a projects the Pareto surface (representing the optimal solutions for the three *OF*'s) on the two-dimensional surface, with the isolines of drip-line distance (*L*) representing the optimal solutions for each specific *L*. Hence, Fig. 4a and b presents identical data, with the isoline of *L* = 40 cm (smallest drip-line spacing) of Fig. 4a corresponding with the Pareto front of Fig. 4b. The solid lines of Fig. 4b–d define

Table 3
Example scenarios of sensitivity analysis.

Analysis		Root distribution	Soil texture	Parameter included in the objective functions		
Type	Scenario			OF_1	OF_2	OF_3
Irrigation system	*I*1	Uniform	Loam	*L*, *D*	*AW*, *DP*	T_a
	*I*2	Uniform	Loam	*L*	*AW*, *DP*	T_a
	*I*3	Uniform	Loam	*L*	*AW*	T_a
Root distribution	*R*1	Uniform	Loam	*L*	*AW*	T_a
	*R*2	Linear	Loam	*L*	*AW*	T_a
Soil texture	*T*1	Uniform	Sandy loam	*L*	*AW*	T_a
	*T*2	Uniform	Loam	*L*	*AW*	T_a
	*T*3	Uniform	Clay loam	*L*	*AW*	T_a

the so-called Pareto fronts that represent the trade-offs between respective objective functions.

In Fig. 4a the Pareto contour plot shows the trade-off between T_a and *AW*, with the contour lines representing isolines of drip-line distance, *L*. For example, Fig. 4a shows that for a given *L* value, larger T_a values will require supplying more *AW* to minimize soil water stress. Moreover, to maintain identical T_a values, values of *AW* must increase as *L* is larger. Specifically, the trade-off in Fig. 4b shows that increasing the AW/T_p ratio from 95% to 110% increases the value of T_a/T_p from 85% to 94%. However, a further increase of *AW* is much less sensitive to T_a, as optimum soil moisture conditions will remain. The results of Fig. 4b are consistent with Fig. 4c, presenting the tradeoffs between root water uptake, as represented by T_a/T_p and drip-line distance, indicating that T_a is increasingly reduced as drip-line distance is increased. By changing drip-line distance from 40 to 140 cm, the T_a value reduces very little, but an additional increase of drip-line distance to 240 cm reduces the relative T_a by about 10%.

When considering Fig. 4d, comparing tradeoffs between *L* and AW/T_p, we note that increased irrigation water applications are needed with increasing distance between drip-lines. This is to be expected as more irrigation water is required to refill soil water storage between irrigation events with increasing distance between irrigation drip-lines. The Pareto front signifies the trade-off between *L* and *AW*. For example, large values for *L* result in low values for OF_1 and high values of OF_2 (Eq. (9)), as more *AW* must be supplied to minimize soil water stress and to maximize T_a. In contrast, by the same reasoning, low *L*-values result in larger values for OF_1 and low values of OF_2. Consequently, the two extreme choices of *L* produce about identical values for the total *OF* value, thereby defining the Pareto front.

3.1. Example scenarios

As before, the Pareto points that exceeded the wetness and transpiration constraints were excluded from further analysis. Thus, for each different scenario the trade-off of applied water (*AW*) and drip-line distance (*L*) are presented, whereby each point of the presented bi-criterion plots corresponds to different Pareto solutions. To better illustrate the effect of drip-line depth (*D*), we used different symbols for the various drip-line installation depth classes for all bi-criterion plots of Fig. 5 (*I*-scenarios), 6 (*R* scenarios), and 9 (*T* scenarios). We also presented the Pareto contour plot of each scenario showing the trade-offs between drip-line installation distance, *L* (OF_1), and applied irrigation water, *AW* (OF_2) with the contour lines representing isolines of alfalfa transpiration, T_a (OF_3).

3.1.1. Irrigation systems – *I*1–*I*3

A comparison of scenarios *I*1 with *I*2 and *I*3 is presented in Fig. 5, for the case of a uniform alfalfa root distribution in a loamy soil. The plots 5a–c summarize the effect of different drip-line installation depths, *D*, on the Pareto distributions for *AW* and drip-line

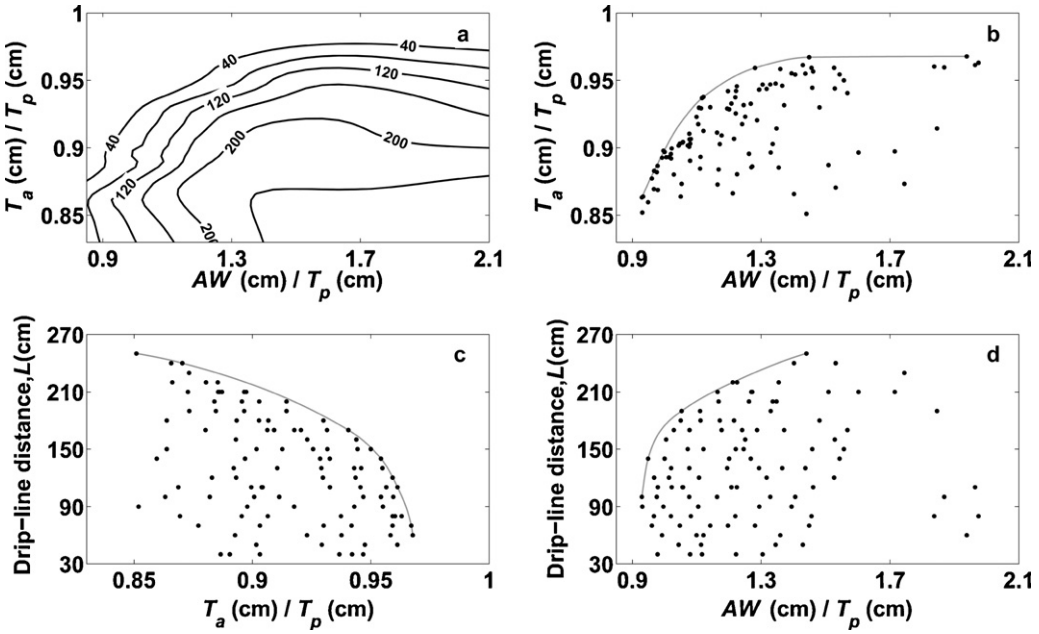

Fig. 4. (a) Pareto contour plot of objective functions in Eq. (9), showing the trade-off between relative transpiration and *AW*, with the contour lines representing isolines of drip-line distance. The other three graphs are corresponding two-dimensional bi-criterion plots for (b) relative transpiration (T_a/T_p) and (AW/T_p), (c) relative transpiration (T_a/T_p) and drip-line distance (*L*), and (d) drip-line distance (*L*) and (AW/T_p).

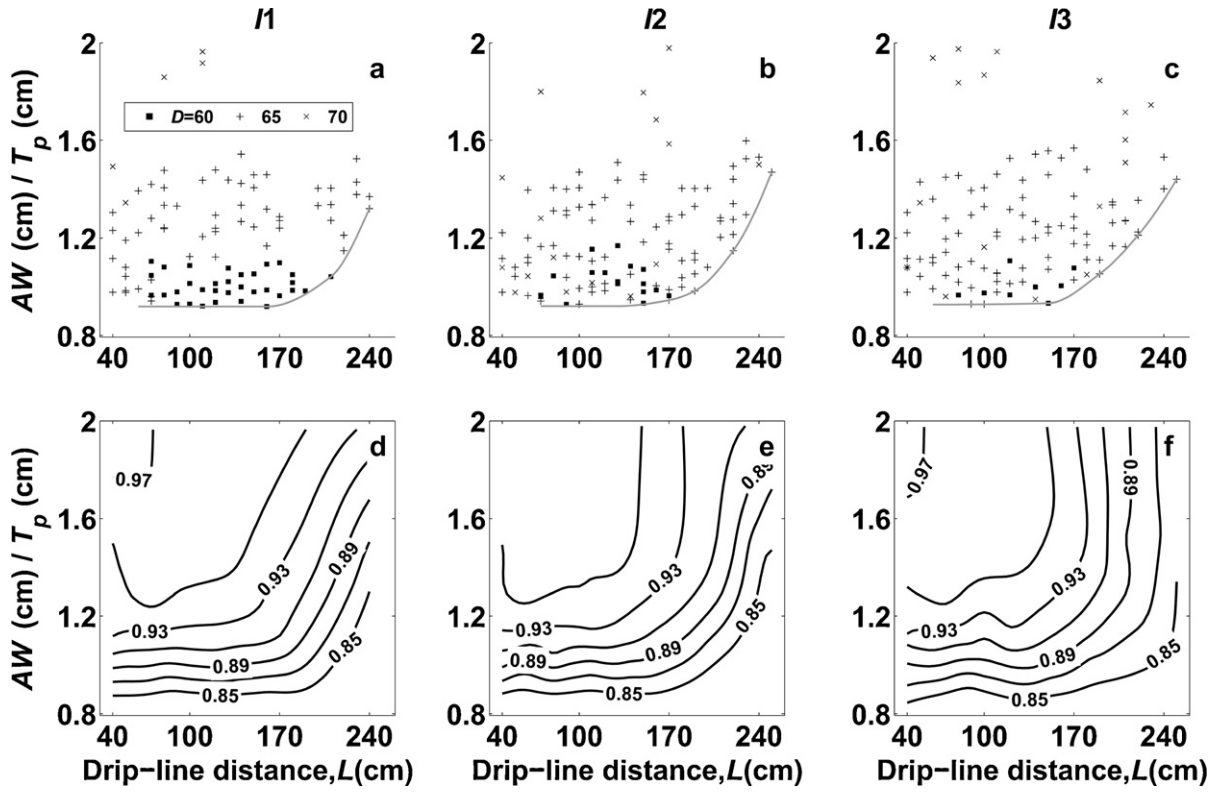

Fig. 5. Bi-criterion (top) and Pareto contour (bottom) plots for *I*-scenarios, optimizing *AW* and drip-line distance, *L*, for (a and d) *I*1, including *D* and *DP* as optimization parameters, (b and e) *I*2, excluding *D* and including *DP* as optimization parameters, and (c and f) *I*3, excluding both *D* and *DP* as optimization parameters. The drip-line depths in plots a–c are indicated with different symbols. The contour lines in plots d–f represent isolines of relative transpiration (T_a/T_p).

distance, *L*. We note that for the *I*2 scenario, ω_D is set to zero, and for *I*3 both ω_D and ω_{DP} values in Eq. (8) are set to zero. Similarly, as in Fig. 4, each symbol represents a high-ranked optimum solution from the Pareto set of optimal solutions. Across all 3 scenarios, we find that *AW* must increase as drip-line distance (*L*) increases. The optimization also showed that the shallowest possible installation depth in this study to satisfy the soil wetness constraint was 60 cm for the case of a uniform root distribution and a loamy soil. That is, even for the *I*1 scenario (with drip-line depth, *D*, among the optimized design parameters), no optimal installation depth solution was found for values of *D* close to the soil surface, hence, we presented only results for drip-line installation depths larger than 60 cm.

A comparison of Fig. 5a–c indicates that the Pareto solutions exhibit a tendency towards deeper drip-line installation depths as one compares *I*1 with *I*2 and *I*3, with the number of AMALGAM solutions for the shallow drip-line depth ($D = 60$ cm) decreasing. As expected, the minimum number of optimal solutions for $D = 70$ cm is the largest for the *I*3 scenario, as deep percolation was excluded as a decision parameter for this scenario, thereby allowing for larger drip installation depths.

The corresponding Pareto contour plots are presented in Fig. 5d–f; with the contour lines representing isolines of relative transpiration, T_a/T_p. When comparing Fig. 5a–c with their corresponding contour plots of Fig. 5d–f, we note that the Pareto front of each scenario is represented by the isoline of $T_a/T_p = 0.85$ in the corresponding Pareto contour plot, as this ratio was the minimum allowable transpiration ratio. All Pareto contour plots show clearly that higher transpiration rates are achieved by either increasing *AW* or decreasing *L*, or both.

Overall though, when comparing Fig. 5a–f, relative small differences between the three different scenarios for *D* and T_a were found. This indicates that the selected design parameters *L* and *AW* are sufficient when optimizing SDI for alfalfa for optimum T_a, but with the assumption that *DP* losses are relatively unimportant. Indeed, the selected soil is a homogenous non-layered loam, for which *DP* is relatively small and the installation cost is not significantly affected by varying the installation depth. For coarse-textured or layered soils with dense layers at deeper depths, we expect the results to be different for the *I*2 and *I*3 scenarios. For these types of soils it is rather difficult to maintain favorable soil moisture conditions required to maximize alfalfa yield and simultaneously minimize deep water percolation. Therefore, *DP* is likely to vary considerably between parameter combinations, and for other than fine textured soils, this variable will become much more important relative to rooting and drip-line installation depths. Alternatively, it is possible to assign an appropriate cost value for deep percolated water and installation depth in Eq. (8), thereby signifying their importance in managing drip irrigation systems.

3.1.2. Root distribution – R1 and R2

The depth distribution of alfalfa roots, in relation to drip-line depth and drip-line distance will largely affect the soil water distribution in the root zone, as it will determine spatial distribution of root water uptake, soil water stress, and *DP* out of the root zone, and thus affecting irrigation system design and management. We therefore analyze the effect of two root distribution types (*R*1, uniform; and *R*2, linearly decreasing) on irrigation system design and management parameters (Fig. 6). In addition, we address the effect of root distribution on soil water and root water uptake dynamics for a given irrigation system (Fig. 7).

3.1.2.1. Analysis of irrigation system parameters. The effect of the two root distribution models (uniform and linear) on the design and management of SDI system is presented in Figs. 6a and b for (*R*1)

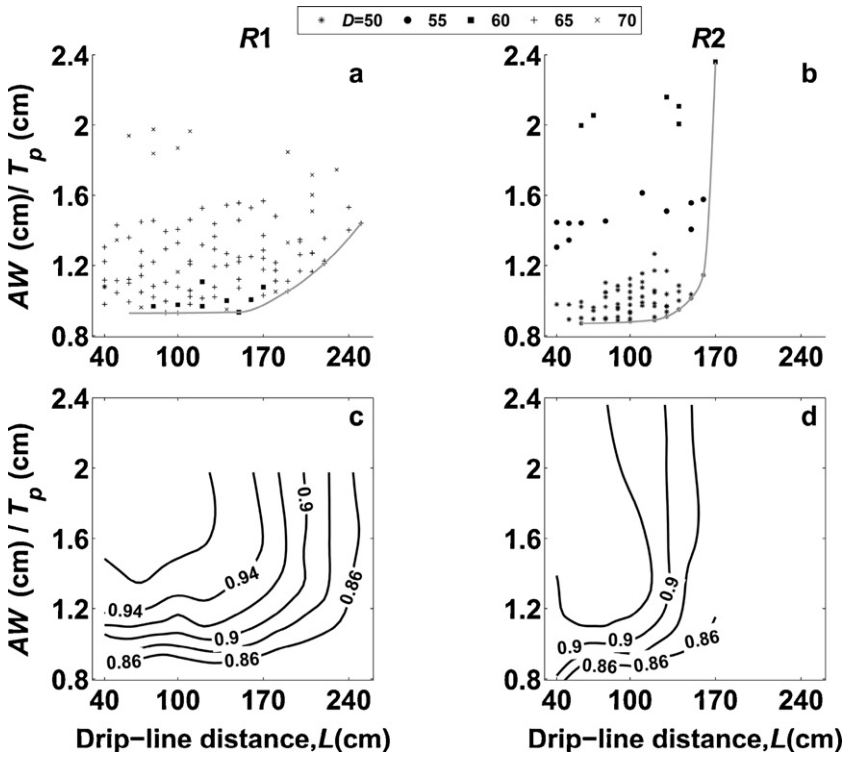

Fig. 6. Bi-criterion (top) and Pareto contour (bottom) plots for *R*1 and *R*2, optimizing *AW* and drip-line distance, *L*, for (a and c) *R*1, uniform root distribution, and (b and d) *R*2, linearly decreasing root distribution. The drip-line depths in plots a and b are indicated with different symbols. The contour lines in plots c and d represent isolines of relative transpiration (T_a/T_p).

uniform and (*R*2) linearly decreasing root system. The bi-criterion graphs illustrate the properties of the Pareto front for drip-line distance (*L*) and applied water (*AW*) for drip-line installation depth (*D*) values ranging between 50 and 70 cm. Moreover, the contour plot of alfalfa relative transpiration, T_a/T_p, representing the trade-offs between drip-line distance, *L*, and irrigation applied water, *AW*, for both *R*1 and *R*2 scenario are presented in Fig. 6c and d. These plots convincingly show that larger values of *L* (cheaper irrigation system) can be compensated for by larger values of *AW*, thereby minimizing soil water stress. For the uniform root distribution results (Fig. 6a, *R*1), none of the Pareto solutions derived with AMALGAM with a drip line installation depth (*D*) of less than 60 cm satisfy the soil dryness constraint at harvesting times. This also explains why the optimal *AW* values generally increase as drip-line

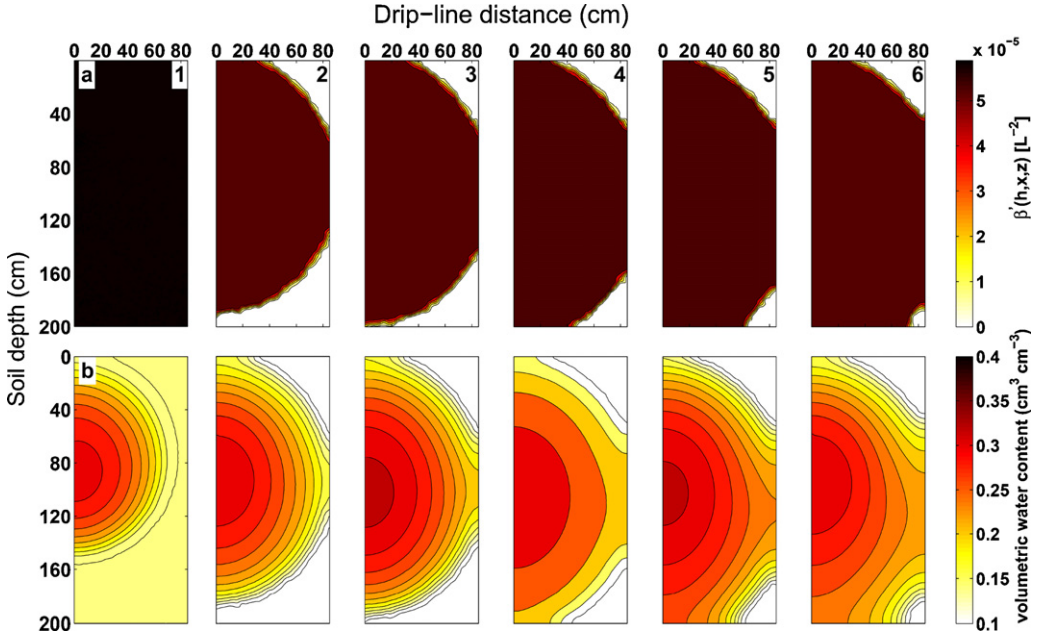

Fig. 7. Spatial distribution of (a) actual root water uptake distribution (β', [L^{-2}]) and corresponding volumetric water content (b) for *R*1 scenario (uniform root distribution), with columns representing the times in the middle of each of the six different cutting cycles (cutting cycle is indicated in the top-right corner). The drip-line is installed at the 60 cm depth.

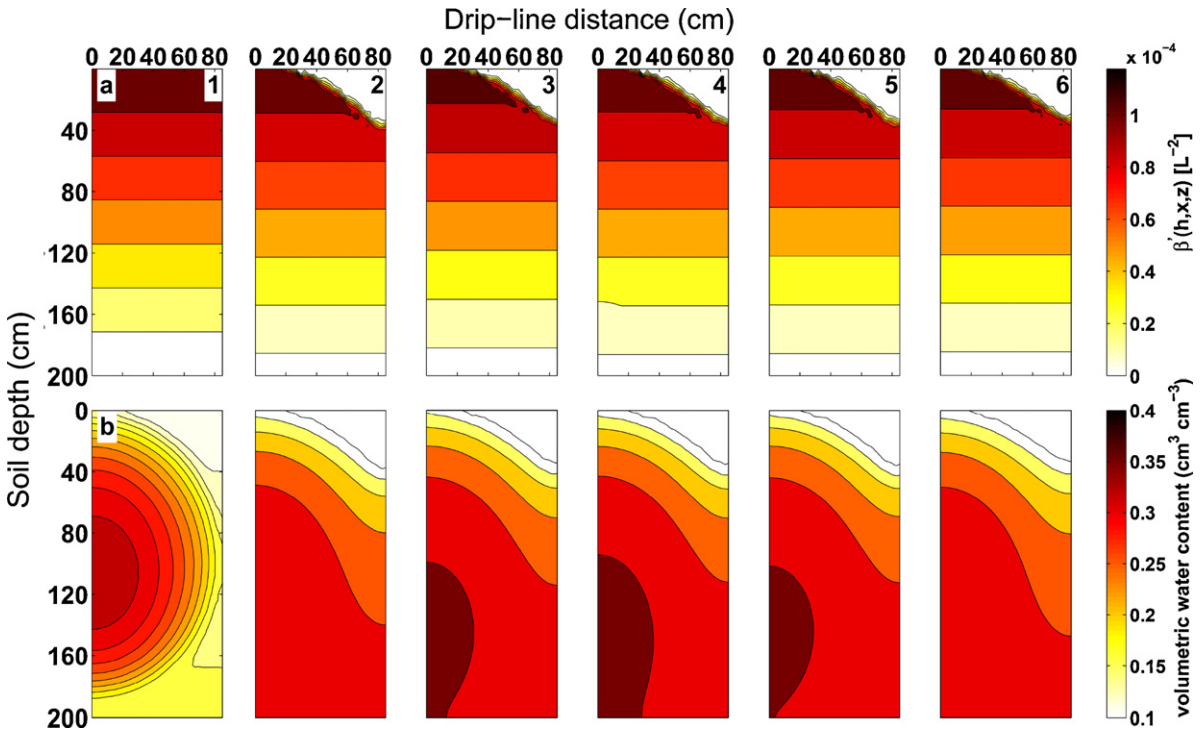

Fig. 8. Spatial distribution of (a) actual root water uptake distribution (β', [L^{-2}]) and corresponding volumetric water content (b) for *R*2 scenario (linear decreasing root distribution), with columns representing the times in the middle of each of the six cutting cycles (cutting cycle is indicated in the top-right corner). The drip-line is installed at the 60 cm depth.

installation depth increases, simply to minimize soil water stress. Similarly, as in Fig. 5, increasing the drip-line distance will lead to an increase in *AW*. This highlights a general finding of our paper, and demonstrates that by increasing the distance between the drip lines (less costly irrigation system) additional applied irrigation water is required to maintain adequate soil moisture conditions in the rooting zone to maximize yield. This trade-off is intuitively clear, and advocates the use of the joint AMALGAM and HYDRUS-2D framework considered herein to find optimal irrigation practices and simultaneously satisfy specific constraints imposed by the farmer.

In contrast to the optimization results of *R*1, the scenario with a linearly decreasing rooting system (*R*2, Fig. 6b), allows for a shallower drip-line installation depth (*D*) of 50 cm, as the maximum root activity at the near soil surface provides for intermittent periods of soil surface dryness. Moreover, the increasing soil water availability with the shallower installation depths minimizes soil water stress as most roots are located near the soil surface. Alternatively, increasing the drip-line installation depth for scenario *R*2 enhances irrigation water losses by *DP*. Therefore, the optimization results in Fig. 6b show that there are no optimal irrigation systems for *D*-values larger than 60 cm. Comparing the alfalfa transpiration (T_a) ranges for *R*1 (Fig. 6c) and *R*2 (Fig. 6d), the results show that a fraction of *AW* is likely available for the higher density of roots in the upper part of the soil profile by capillary rise for $D < 65$ cm. However, this upwards-directed water supply was insufficient for the loamy soil to obtain the T_a as high as that achieved for the uniform root distribution scenario, *R*1. The AMALGAM optimization results show that this upwards-directed water supply was not sufficient to satisfy the prior defined constraints on T_a and thus no optimal solution was found for $D > 65$ cm.

3.1.2.2. Analysis of soil water distribution and root water uptake. As an example, we evaluate the effect of irrigation system parameters for fixed values of drip-line distance ($L = 170$ cm) and drip-line installation depth ($D = 60$ cm). This is the most economic irrigation system design, with maximum spacing of the drip-lines, and nearest drip installation to the soil surface. The optimized irrigation scheduling for this scenario resulted in a single Pareto irrigation interval of two days only, with irrigation duration (*ID*) of 10 and 20 h for root systems *R*1 and *R*2, respectively. To maintain favorable soil moisture conditions and avoid water stress conditions, scenario *R*2 with a linearly decreasing root distribution requires a doubling of irrigation water amounts, *AW*, to maintain similar T_a values. Figs. 7 and 8 present the corresponding spatial distributions of root water uptake (top), as represented by $\beta'(h,x,z)$ of Eq. (6b) and the sink term *S* computed using daily values (day^{-1}), and volumetric soil water content (bottom) for *R*1 (Fig. 7) and *R*2 (Fig. 8). The six different panels represent snapshots at the middle of each of the six different cutting cycles. The spatial patterns or root water uptake are largely determined by the spatial distribution of roots, as defined by $\beta(x,z)$ in Eq. (5), with reductions in uptake caused by the soil water stress function, $\alpha(h)$, in Eq. (4).

For the uniform root distribution (Fig. 7), the roots initially take up water uniformly from the entire soil profile. In later cutting cycles, the uptake rate varies spatially depending on available soil water. For the first three cutting cycles, the soil wetting patterns remain in the center of the soil profile (Fig. 7b), and is symmetric around the drip line ($D = 60$ cm), causing reduced root water uptake at the soil surface and bottom of the soil profile, and possibly some cumulative soil water stress. However, for the latter 3 cutting cycles, soil water redistributes downward by gravity, increasing the wetted soil root zone towards 200 cm, causing water losses by *DP*.

The final optimized results for the *R*2 root system in Fig. 8 show that root water uptake is concentrated in the top of the soil profile (Fig. 8a), as expected, with significant water losses by *DP* (Fig. 8b) for the cutting cycles in mid season (cycles 3, 4, and 5). However, most of the *AW* moves upward by capillary rise as a result of large negative gradients of soil water pressure head close to the surface caused by root water uptake. Maximum root water uptake occurs near the soil surface, since there are relatively fewer roots at and below the

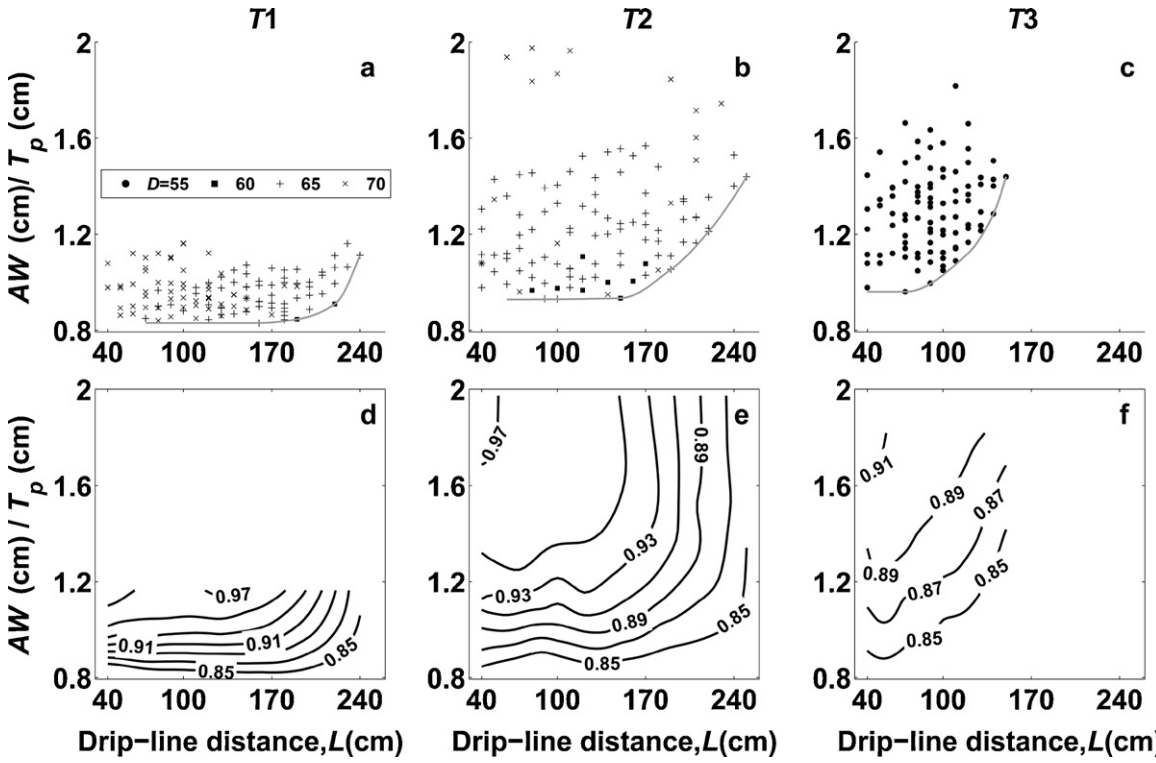

Fig. 9. Bi-criterion (top) and Pareto contour (bottom) plots for *T*1 (clay loam), *T*2 (loam), and *T*3 (sandy loam), optimizing AW/T_p and drip-line distance, *L*, for drip-line installation depths of 55–70 cm. The drip-line depths in plots a–c are indicated with different symbols. The contour lines in plots d–f represent isolines of relative transpiration (T_a/T_p).

drip-line. Since the near-soil surface between the two drip-lines was insufficiently wetted, root water uptake there is rather low, causing soil water stress.

In summary, for the linear root distribution case (*R*2) water is required at shallower depths and in higher amounts as compared to the uniform root distribution (*R*1), thereby leading to significant water losses by *DP*. In contrast, root water uptake is constant and independent of soil depth for *R*1, allowing *AW* to be much lower to maintain adequate root water uptake with no soil water stress. We note that these results may be different if the root water model allows for compensated uptake, as presented in Šimůnek and Hopmans (2009). These results indicate that the root distribution has a major effect on system design and irrigation management.

3.1.3. Analysis of soil texture – T1–T3

The bi-criterion Pareto plots for the clay loam (*T*1), loam (*T*2), and sandy loam (*T*3) soil with uniform root distribution are presented in Fig. 9a–c, respectively. Additionally, the Pareto contour plots of T_a/T_p for each soil type representing trade-off between *L* and *AW* are shown in Fig. 9d–f. No optimal Pareto parameter values were determined for drip-line installation depths of 55 and 60 cm for *T*1 (clay loam) and 55 cm depth for *T*2 (loam), as the finer-textured soils allow for deeper optimum *D*-values because of sufficient water holding capacity and low *DP* losses, while the shallower installations cause too wet soil conditions near the surface at harvesting. Because of its higher water holding capacity, much lower *AW is* required for the clay loam than the loam soil to achieve high transpiration rates (Fig. 9d–e). However, for the sandy loam soil, all of the Pareto solutions were determined from the shallow drip-line installation at *D* = 55 cm, as it is a well-drained soil that satisfies the soil dryness constraint, while simultaneously minimizing *DP*. Although, drip-line installation at *D* = 55 cm was sufficient for AMALGAM to find Pareto solutions for the sandy loam soil, it is shown in Fig. 9f that the soil water holding capacity was not enough to avoid soil water stress and thus lower transpiration obtained compared to those achieved for the loam and clay loam soils, especially at the larger drip-line distances. As Fig. 9 shows, the finer-textured soils of *T*1 and *T*2 allow for drip-line installation depths of 70 cm, as *DP* losses are relatively small, while maintaining dry soil surface conditions. When comparing the Pareto contour plot of scenarios *T*1–*T*3 it is shown that larger amounts of *AW* are required to maintain a specified transpiration rate as the soil texture is coarser, as corresponding soil water holding capacity decrease and *DP* losses increase.

When comparing optimal drip-line distance (*L*) between the various soil types, the results show that larger *L*-values are possible for finer-textured soils (compare *T*3 with *T*1) for any given installation depth, *D*. This is so because the lateral soil water movement in clay loam (*T*1) is larger as compared to the sandy loam soil (*T*3). However, the increasing capillary rise for the clay loam soil maintains a wet soil near the soil surface, thereby eliminating the possibility of shallow drip line installation depths for soil types *T*1 and *T*2.

4. Conclusions

An irrigation design-management modeling tool was developed to simultaneously optimize subsurface drip irrigation system design and management, using the optimization model AMALGAM. With this multi-criteria optimization approach, in combination with HYDRUS-2D modeling to simulate unsaturated soil water flow and root water uptake, the presented sensitivity analysis provides for optimal irrigation system and management parameters for a wide range of conditions, including drip-line installation depth and distance, applied irrigation water, degree of crop water stress, and drainage losses. The so-called optimal Pareto solutions suggest multiple trade-offs, depending on the specific parameter of most interest. Though not explicitly presented, the proposed

optimization scheme with multiple objective functions allows for inclusion of costs for the different irrigation systems and management practices, thereby allowing for an economic analysis as well.

The importance of root distribution in irrigation system design and water management has been acknowledged for several decades, and has been evaluated by consideration of two different depth distribution functions of root architecture. We concluded that root distribution has a large effect on optimal applied irrigation water, irrigation water scheduling, and deep percolation losses. Also, we recognize the general lack of information on the effects of irrigation type on alfalfa root distribution, necessitating dedicated experiments to determine the influence of subsurface drip on root growth and spatial distribution.

Analysis of the soil texture effects showed major differences because of variations in water holding capacity, capillary forces and drainage rates between soil types. Consequently, the number of combinations of optimal Pareto parameter values was limited for the coarse-textured soils because of increasing deep drainage losses, whereas optimal solutions were limited to deeper drip-line installation depths for the finer-textured soils because of upward capillary gradients thereby preventing dry soil surface conditions required for alfalfa harvesting.

The study presents examples of the capabilities of flexible irrigation design-management tool for alfalfa, but can be equally applied to other crops and climates. Moreover, the presented framework can be utilized to include cost estimates to the multi-criteria objective functions, thereby allowing for an extensive economic cost-benefit analysis for a range of irrigation system designs and irrigation water management practices.

Acknowledgements

This project was partly possible through a graduate student fellowship by the Hydrologic Sciences Graduate Group at UC Davis. The AMALGAM source code can be obtained from the third author upon request.

References

Abdul-Jabbar, A.S., Sammis, T.W., Lugg, D.G., 1982. Effect of moisture level on the root pattern of alfalfa. Irrig. Sci. 3 (3), 197–207.

Alam, M., Trooien, T.P., Dumler, T.J., Rogers, T.H., 2002. Using subsurface drip irrigation for alfalfa. J. Am. Water Resour. Assoc. 38 (6), 1715–1721.

Alfalfa fact sheet composed by the California Foundation for Agriculture in the Classroom, 2011. Available online at (http://www.cfaitc.org/factsheets/pdf/Alfalfa.pdf). Checked on 12.01.2012.

Allen, R.G., Pereira, L.S., Raes, D. and Smith, M., 1998. Crop evapotranspiration guidelines for computing crop water requirements. FAO Irrigation and Drainage Paper No. 56, United Nations – Food and Agricultural Organization, Rome, Italy, p. 300.

ASCE EWRI, 2005. The ASCE Standardized Reference Evapotranspiration Equation. Environmental and Water Resources Institute (EWRI) of the American Society of Civil Engineers Task Committee on Standardization of Reference Evapotranspiration Calculation, ASCE, Washington, DC, p. 70. Available online at (http://www.kimberly.uidaho.edu/water/asceewri/ascestzdetmain2005.pdf). Checked on 12.01.2012.

Breazeale, D., Neufeld, J., Myer, G., Davison, J., 2000. Feasibility of subsurface drip irrigation for alfalfa. J. ASFMRA, 58–63.

Carsel, R.F., Parrish, R.S., 1988. Developing joint probability distributions of soil water retention characteristics. Water Resour. Res. 24, 755–769.

Doorenbos, J. Pruitt, W.O., 1977. Crop water requirements. Revised 1977. FAO Irrigation and Drainage Paper No. 24, United Nations – Food and Agricultural Organization, Rome, Italy, p. 144.

Feddes, R.A., Kowalik, P., Kolinska-Malinka, K., Zaradny, H., 1976. Simulation of field water uptake by plants using a soil water dependent root extraction function. J. Hydrol. 31, 13–26.

Gärdenäs, A.I., Hopmans, J.W., Hanson, B.R., Šimůnek, J., 2005. Two-dimensional modeling of nitrate leaching for various fertigation scenarios under micro-irrigation. Agric. Water Manage. 74 (3), 219–242.

Godoy, A.C., Pérez, G.A., Torres, E.C.A., Hermosillo, L.J., Reyes, J.e.I., 2003. Water use, forage production and water relations in alfalfa with subsurface drip irrigation. Agrociencia 37, 107–115.

Grismer, M.E., 2001. Regional alfalfa yield, ET_c, and water value in western states. ASCE 127 (3), 131–139.

Hanson, B.R., Šimůnek, J., Hopmans, J.W., 2006. Evaluation of urea–ammonium–nitrate fertigation with drip irrigation using numerical modeling. Agric. Water Manage. 86 (1–2), 102–113.

Hanson, B.R., Šimůnek, J., Hopmans, J.W., 2008. Leaching with subsurface drip irrigation under saline, shallow ground water conditions. Vadose Zone J., doi:10.2136/VZJ2007.0053, Special issue "Vadose Zone Modeling" 7(2), 810–818.

Huisman, J.A., Rings, J., Vrugt, J.A., Sorg, J., Vereecken, H., 2010. Hydraulic properties of a model dike from coupled Bayesian and multi-criteria hydrologeophysical inversion. J. Hydrol. 380, 62–73.

Hutmacher, R.B., Phene, C.J., Mead, R.M., Shouse, P., Clark, D., Vail, S.S., Swain, R., Peters, M.S., Hawk, C.A., Kershaw, D., Donovan, T., Jobes, J., Fargerlund, J., 2001. Subsurface drip and furrow irrigation comparison with alfalfa in the Imperial Valley. In: Proc. 2001 California Alfalfa & Forage Symposium, Modesto, CA, 11–13 December, p. 2001.

Meinzer, O.E., 1927. Plants as indicator of ground water. United States Geological Survey Water-Supply Paper 577.

Natural Resources Defense Council, 2001. Alfalfa-the thirstiest crop. California's antiquated water policy allows large corporate farms to grow too much water-hogging alfalfa. Available online at http://web.archive.org/web/20010702041017/http://www.nrdc.org/water/conservation/fcawater.asp). Checked on 12.01.2012.

Putnam, D.H., Russelle, M., Orloff, S., Kuhn, J., Fitzhugh, L., Godfrey, L., Kiess, A., Long, R., 2001. Alfalfa, Wildlife and the Environment—The importance and Benefits of Alfalfa in the 21st Century. California Alfalfa and Forage Association, Novato, CA, 24 pages.

Šimůnek, J., Šejna, M., van Genuchten, M.Th., 2006. The HYDRUS software package for simulating two- and three-dimensional movement of water, heat, and multiple solutes in variably-saturated media. Technical Manual, Version 1.0, PC Progress, Prague, Czech Republic.

Šimůnek, J., van Genuchten, M., Šejna, M.Th., 2008. Development and applications of the HYDRUS and STANMOD software packages, and related codes. Vadose Zone Journal 7 (2), 587–600.

Šimůnek, J., Hopmans, J.W., 2009. Modeling compensated root water and nutrient uptake. Ecol. Model. 22 (4), 505–521.

Skaggs, T.H., van Genuchten, M.Th., Shouse, P.J., Poss, J.A., 2006. Macroscopic approaches to root water uptake as a function of water and salinity stress. Agric. Water Manage. 86, 140–149.

Snyder, R.L., Bali, K.M., 2008. Irrigation scheduling of alfalfa using evapotranspiration. In: Proc. 2008 California Alfalfa & Forage Symposium and Western Seed Conference, San Diego, CA, 2–4 December, p. 2008.

Taylor, S.A., Ashcroft, G.M., 1972. Physical Edaphology. Freeman and Co., San Francisco, California, pp. 434–435.

van Genuchten, M.Th., 1980. A closed-form equation for predicting hydraulic conductivity of unsaturated soils. Soil Sci. Soc. Am. J. 44, 892–898.

Vrugt, J.A., Robinson, B.A., 2007. Improvement evolutionary optimization from genetically adaptive multimethod search. Proc. Natl. Acad. Sci U.S.A. 104 (3), 708–711.

Vrugt, J.A., Robinson, B.A., Hyman, J.M., 2009. Self-adaptive multimethod search for global optimization in real-parameter spaces. IEEE Trans. Evol. Comput. 13 (2), 243–259.

Wöhling, T., Vrugt, J.A., Barkle, G.F., 2008. Comparison of three multi-objective optimization algorithms for inverse modeling of vadose zone hydraulic properties. Soil Sci. Soc. Am. J. 72 (2), 305–319.